Building a Bench with Magnetic Bearings for Study of Rotor Dynamics

Jefferson S. Coelho[1] and Fernando Augusto N. C. Pinto[2]

[1] Federal University of Amazonas, Amazonas, Brazil
jeffersoncoelho@ufam.edu.br
[2] Federal University of Rio de Janeiro, Rio de Janeiro, Brazil.
fcpinto@ufrj.br

Abstract

Along with the rise of great technological advancements came new products and processes, demanding an increase in quality and production growth. This work presents a study on Active Magnetic Bearings, a no contact, friction-free device that supports a rotor through magnetic forces. Thus, a few of its advantages include a low maintenance cost and the possibility of working at high rotation speeds. A disadvantage is the need for a control loop. Therefore, a PID controller is implemented on an embedded electronic FPGA-based platform reconfigurable for levitation, stabilization and the analysis of the rotor's dynamic behavior. To achieve the proposed objective, a prototype of the system was developed to carry out measurements and experimental analyses and to observe the advantages and disadvantages offered by the system. The results obtained show that the rotor maintains itself within the acceptable displacement zone around the bearings' geometric center. Therefore, the controller managed to stabilize the system so its dynamic behavior does not exceed the limit established in this project.

Contents

1 Introduction

Rotating machines have tendency to work in increasingly severe conditions, with high spin speeds and high load values applied, even maintaining the high standard demand in productivity and reliability [17]. Therefore, there is need for modifications and improvements in the machine

designs so that they can meet the new performance standards and with high efficiency. An example in modern industry is compressors [2]. These are used in applications that require pressurization of gases or liquids, for example, in the petrochemical industry. In oil exploration in deep or ultra-deep waters (pre-salt layer) where high pressures occur, compressors are not easily accessible for diagnosis and frequent maintenance. dog. Therefore, it becomes necessary equipment with a high technological level that can work for long periods of time without maintenance, efficiently and with great reliability. Rotating machines such as pumps, electric motors and generators, compressors, steam turbines, gas, are basically formed by three main components: the rotor, the bearings and the support structures [6]. The bearings are responsible for supporting loads and also guiding the axes even in the presence of external forces, such as, for example, vibrations due to rotor unbalance. In this scenario, the bearings are presented as important parts, which inuence the dynamic performance of the rotor, life and reliability of the machine.

Recent developments in electronics have increased the need for advanced electronic control systems, due to the increased capacity and speed of digital platforms such as Digital Signal Processors (DSP), microcontrollers, FPGA (Field Programmable Gate Array) high-performance, Application-specific integrated circuits (ASICs), among others. Thus, active magnetic bearings (AMBs) have gained a great ally, as they are systems where they need a control loop for rotor stabilization, as they are unstable in nature. With that, its use became more attractive and serving as an alternative to replace the current conventional bearings in modern machines due to the advantage of the complete elimination of the mechanical contact between the rotating parts and the fixed parts . Its operating principle is based on the use of forces from magnetic fields, produced by electromagnets, to maintain to maintain relative position of a rotating assembly (rotor) to a stationary component (stator), providing high rotation speeds, absence of lubrication, longer service life and lower maintenance cost [19]. For Yoon [20], these are highly desirable features for compressors. Other advantages that we can mention are in relation to the monitoring and diagnosis of systems during the machine operation [10], this can be designed for analysis and interpretation of measurement data that are collected through sensors arranged in the bearings, making it possible to modify the dynamic characteristics, such as stiffness and damping [11]. Some application areas with active magnetic bearings can be found in [14], such as: turbomachinery [1], energy storage system (Flywhells) [7], Biomedical [8], Oil and Gas [5, 16].

One of the greatest challenges in the use of AMBs is to control and stabilize the rotor, so that it can support loads and guarantee a good dynamic behavior against high rotation speeds and disturbances that can occur. For this, new control strategies that can meet these needs must be developed and tested. The main aim of this study is to investigate dynamic behavior of the magnetic bearing system, evaluating the characteristics of the response for cases where the rotor is subject to a static (no rotation), transient, dynamic (with rotation) and with perturbations.

2 Active Magnetic Bearing System Design

The test rig consists of a shaft/rotor supported by two radial AMBs, polypropylene plate to limit the radial movement of the rotor and also as protection of the stator or rotor surface due to eventual failures, and support axial to avoid movement in the longitudinal direction. The AMB system is composed of position sensors, power amplifiers, on-board controller responsible for signal processing, and a drive system through a DC motor (Direct Current), whose speed control is done through a PWM signal (Pulse Width Modulation) and measured with the aid of a digital tachometer. These elements can be identified in Figure 1.

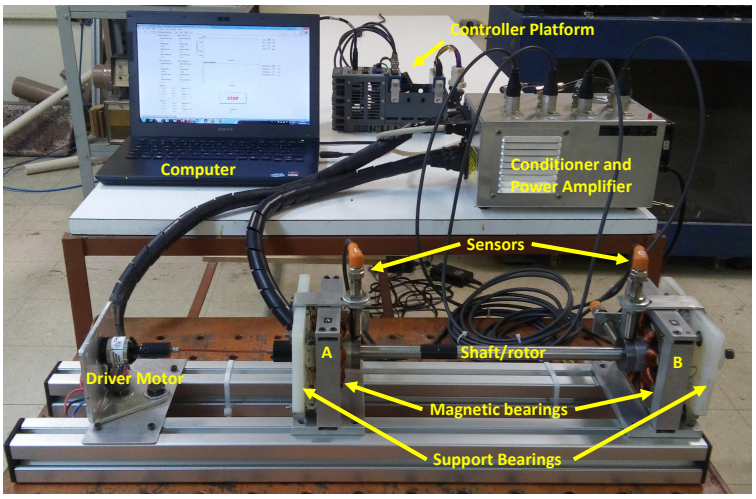

Figure 1: Assembled AMB test rig.

Table 1 the main constructive parameters of the AMB system are presented.

Parameter	Value	Unit
Number of coil turns per pair	260	–
Resistance of each coil pair	$1,2$	Ω
Base current in the coils	$1,0$	A
Rotor/Bearing Clearance (gap)	$1,0$	mm
Rotor Clearance/Support	$0,5$	mm
Shaft length	400	mm
Shaft/rotor assembly mass	$1,0$	kg
Distance between bearings	315	mm

Table 1: AMB System Parameters.

The assembly of the bearings was built on a structural aluminum profile in order to keep the components centralized and aligned, however, an assembly that meets these conditions is almost impossible. One of the advantages that was observed in the prototype is that the magnetic bearings have mechanical characteristics where it is possible to adjust the control for proper functioning. The AMB system has a platform where they were allocated the power sources of the sensors and power system. This platform is internally composed of a $12V/20A$, a font of $24V$, four power controllers, circuit for conditioning the sensor signal and serial port for connection with controller platform (Compact-RIO).

2.1 Magnetic Bearing

The constructive aspects of the prototype with its structure and materials used in the mechanical design of the magnetic bearing are presented. The Electromagnet shows Figure 2 two It is composed of a stator (ferromagnetic core) and electrical coils.

The stator has a heteropolar configuration that is the most used, where the magnetic field travels radially. The sheet material used was non-oriented grain silicon steel with thicknesses

of $0.5mm$ due to its magnetic properties such as high permeability and mainly high magnetic saturation. These characteristics were obtained from the BH magnetization curve described by [15].

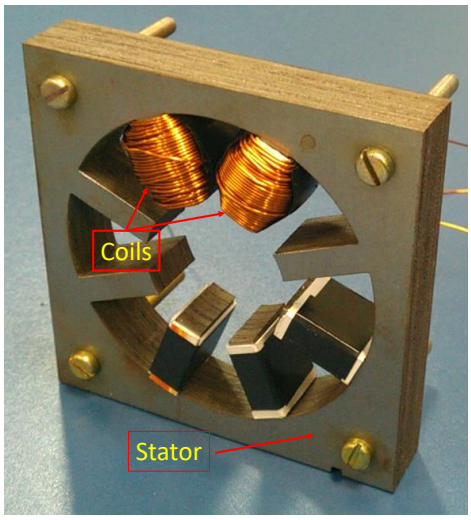

Figure 2: Stator and coils set.

The coil is made of a copper conductor covered by a thin insulating enamel layer, gauge AWG22 ($0.33mm^2$), wound with 130 turns per tooth, totaling 260 per pair of coils, providing a maximum current of $10A$.

2.2 Rotor

The rotor consists of a set of blocks that will be fitted to the shaft, these are composed of three discs. The first disc is made of carbon steel and has the function of supporting the other discs and serving as a surface for reading the sensors. The second disc is made of aluminum, whose function is to move the sensors away from the coils actuation site and prevent it from interfering with the reading, in addition to creating a necessary physical spacing When mounting the sensor with the bearing. Finally, the last disc is made up of a set of plates of the same material used in the stator, nonoriented grain silicon steel, with a good surface finish, concentricity and uniform diameter to ensure a good alignment with the bearing stator. The main shaft is made of stainless steel due to its mechanical resistance property, its length is $40mm$, with $14.28mm$ of diameter. Figure 3 shows the complete rotor.

Figure 3: Shaft-Rotor set.

2.3 Sensors

The position sensors used are of the inductive type and provide an analog output signal in voltage that varies linearly between $0V$ and $10V$ proportional to the distance measured in the air gap, with a measuring range of $0.2mm$ to $2mm$ and noise of approximately $3\mu m$. Its operation is more compatible with what is desired and its measurement is the least influenced by external agents [3]. A total of four sensors were mounted in the radial directions of the two bearings, with two sensors per bearing (one in the horizontal direction and one vertically perpendicular to each other) to measure the position without mechanical contact with the shaft.

The bearing has a nominal air gap of $1.0mm$ radial with the rotor at the operating point. In this way, the rotor can move radially in a range from 0 to 2.00 mm. However, the maximum movement clearance is given by the support bearing, whose function is to avoid contact between the rotor and the bearing in case of malfunction. In this case, the clearance between the rotor and support is $0.5mm$, therefore, the radial displacement region of the rotor starting from the operating point is from 0 to $1.0mm$. During the installation of the sensors, a displacement of $1.1mm$ was considered between the sensor and rotor from the operating point. Thus, the operating range of the sensors varies from 0.5 to $1.6mm$. Figure 4 shows the mounted sensors on the bearing and rotor.

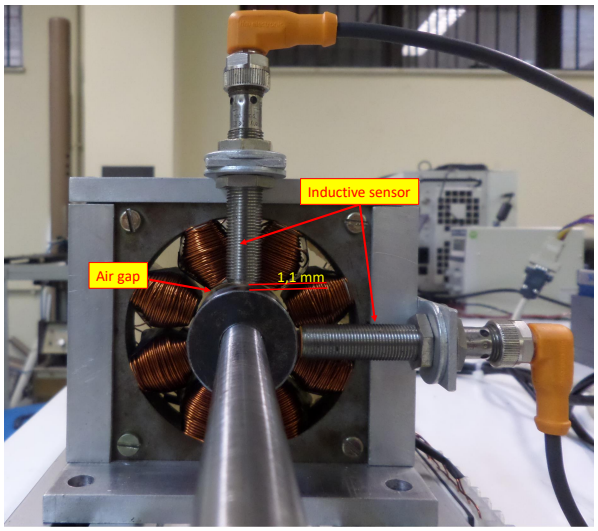

Figure 4: Inductive position sensor.

2.4 Electronic Power System

The purpose of the electronic power system is to transform the weak control output signal, into voltage, into current that flows through the bearing coils, and thus provide the necessary force to suspend the rotor. The system used is a board Monster Moto Shield gives Sparkfun Electronics which has a pair of VNH2SP30 full bridge controllers capable of controlling high currents independently (Figure 5). The integrated circuit board of the controller has an internally switched amplifier with a full H-bridge, which can supply up to $14A$ of direct current and PWM frequency of up to $20kHz$. Although the system has a complete H-bridge in the magnetic

bearing, only half a bridge was used, as it is not necessary to invert the direction that the current flows through the coil.

Figure 5: Electronic Power System [18].

For more precise control of the bearing current, the PWM technique was used, where the output of the control signal determines the pulse width, or duty cycle, and is directly related to the voltage average. This signal will be transferred to the digital controller with a PWM frequency of $10kHz$ at the output and applied to the input of the power amplifier (bridge H) used to control the current value in the coils. In total, four devices were used, each of which controls a shaft with two bearing directions.

2.5 Acquisition and Control System

The controller platform used is the compactRIO 9030 from National Instruments. It features $1{,}33GHz$ dualcore Intel Atom processorGHz, 4 GB non-volatile storage, 1 DDR3 memoryGB, and 4 compartments for input and output modules (analog or digital). The controller operates with an embedded processing system running LabVIEW Real-Time for control, data acquisition and analysis. The platform chassis is where the input and output modules are assembled and allows communication between these modules and the controller, it integrates a matrix of logic circuits with reconfigured port arrangements (FPGA). This technology provides the reliability of a hardware dedicated and deterministic performance of closed-loop controls at extremely fast rates exceeding $1MHz$ [13].

The control loop implementation was developed with the high-level graphical programming tool based on data flow in LabVIEW where it has function blocks for developing FPGA-based control systems. The programming is done using fixed-point data type, as it can optimize the FPGA resources, and with simple precision floating point. The logic used to implement the PID control is presented in the block diagram in 6. Many control solutions have been used over time, but the PID controller is the most used in the industry today [4]. The block diagram reads the sensor signal inputs, in voltage, is then converted to millimeters, and sent to the PID controller where it compares it to a reference value, then is treated by the law of control. Its control signal will be added and subtracted to a constant value (base value) causing the direction to act in a differential way guaranteeing equal forces in both directions for the coils, these signals of operating mode outputs are sent to a duty cycle input (PWM) on the power

system.

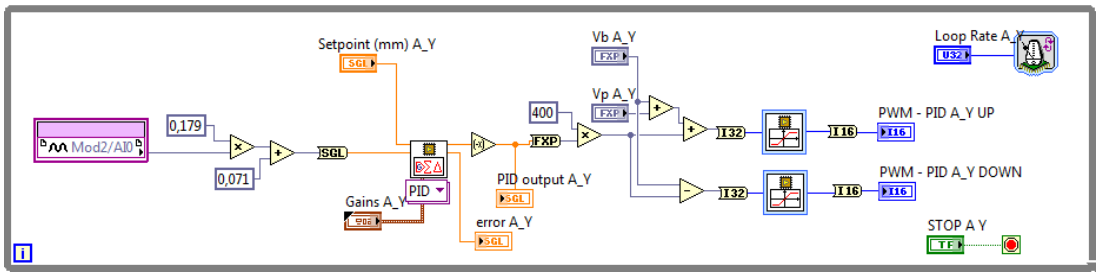

Figure 6: FPGA block diagram for the implementation of the PID controller.

The controller was implemented in FPGA with a sampling frequency of $10kHz$ (100μs) that can be changed. This value was chosen based on the orientations of Schweitzer [14], where they usually use rates between 5 to $10kHz$ for magnetic bearing systems in a digital control implementation.

2.6 Drive System

The bearings are driven by a DC motor from the manufacturer JDrones. Control is done through a PWM signal generated by an embedded device from National Instrument to vary its angular velocity. Figure 7 shows the drive system used. The bearings can be driven by other types of motors according to the application need.

Figure 7: DC motor and speed controller [9].

3 Results

This section aims to present and discuss the experimental results obtained in the prototype of the AMS system. Tests were carried out with different situations, evaluating the following response characteristics: static behavior (without rotation), transient, dynamic (with rotation) and perturbations. The graph of the orbit is presented with the trajectory of the movement of the geometric center of the rotor in the plane xy defined by the position sensors. The orbit provides important information as it represents the real path of the rotor's geometric center during lateral vibrations [12].

3.1 System response during run-up

Initially, the response of the system with the rotor at rest supported by the support bearings was analyzed, and then the system was started. For mechanical purposes, this is important to verify if the system will effectively manage to reach stability within a time interval and the level of disturbance that can occur in the contact of the support bearings with the rotor. In general, analyzing the dynamic behavior of the system during startup means studying the transient response.

Figures 8a and 8a show the changes in rotor displacement in the vertical direction at the time the system is activated. The system stabilized maintaining an oscillation around $0.005mm$ ($5\mu m$) of amplitude. It was observed the rotor is not taken directly to the zero position, taking approximately 2s to reach the steady-state, which is the system's accommodation time. This effect is due to the control system and is related to the integrative term, which has as its main function to eliminate the steady-state error and keep the rotor in the center of the magnetic bearings.

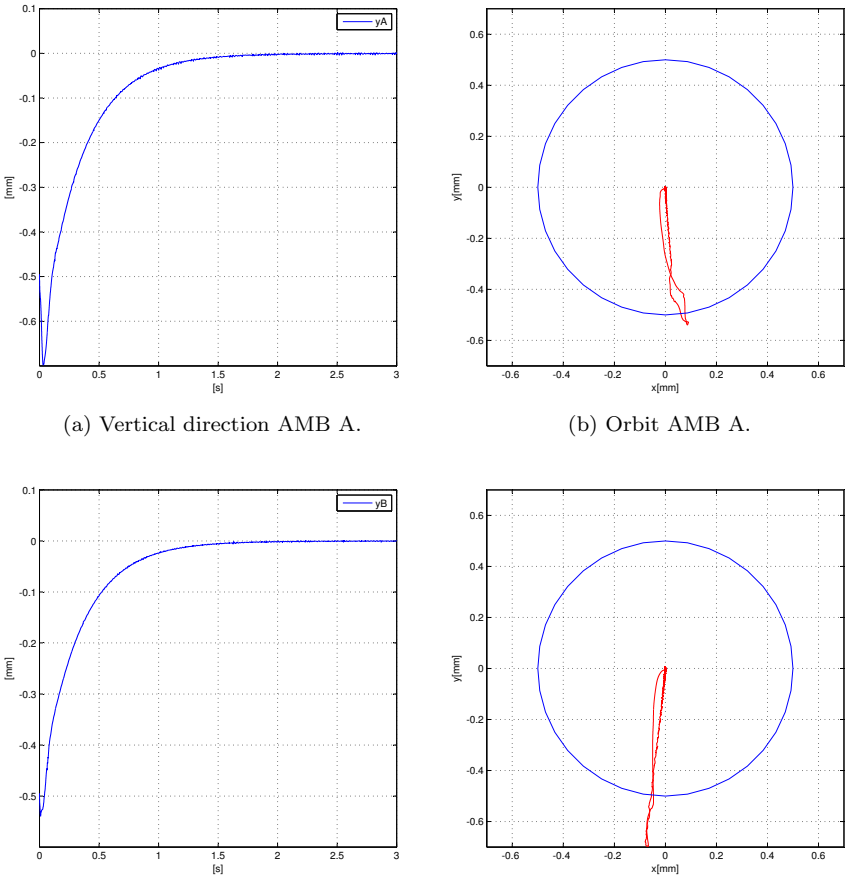

(a) Vertical direction AMB A.

(b) Orbit AMB A.

(c) Vertical direction AMB B.

(d) Orbit AMB B

Figure 8: Transient response of the rotor during run-up.

Figures 8b and 8d the orbits of rotor movement within the bearings are shows. It is verified that the rotor has asymmetrical movements during start caused by the irregular initial position of the rotor inside the support bearing. This could be due to the non-ideal manufacture of the bearing, a possible eccentricity with the stator or also misalignment of the bearings. It is also observed that the displacements are greater than the radial clearance. This may have happened because of the loss of the displacement sensors calibration adjustment due to the rotor vibration in the support bearings during the start, caused by the fact that the sensors are fixed in the support structure and these have been made of elastic material. The results show that even with a non-ideal geometry, the system performed satisfactorily, keeping it stable.

3.2 System response in steady-state

The analysis of the dynamic behavior of the system for an operation with zero rotation speed will be presented. Therefore, the maximum displacement of the shaft in relation to the central position of the bearings will be seen.

Figures 9a and 9b present the graphs of the orbits of the axis put into operation for the system response is measured steady-state. It is observed that the rotor remains most of the time in a range of $0.004mm$ with respect to the zero points, but not being completely static. This was expected, since the system has a decentralized control structure, that is, a controller for each bearing direction acting independently to keep the rotor position stable. However, the vibration produced by the vertical control also influences the horizontal direction. Even with these small displacements, the system presents a satisfactory response indicating an operation with an adequate performance of the control system.

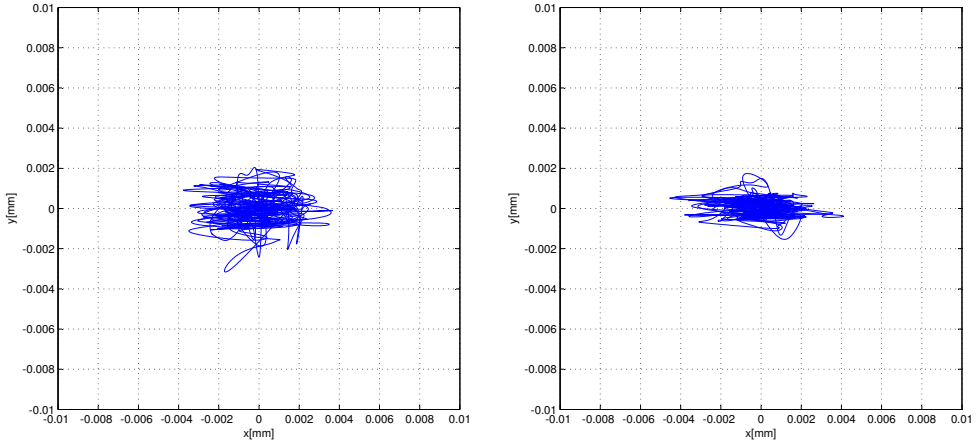

(a) AMB A. (b) AMB B.

Figure 9: Measured rotor orbits (in mm) at radial AMB.

3.3 Rotating system response

The analysis of the dynamic behavior of the system will be done with the rotor rotating at rotation speeds of 2000 and 3000 RPM. The system is driven by a DC motor coupled at the

end of the shaft close to bearing A. Initially, the analysis will be made for the case of the system without unbalancing excitation, only considering the rotor's own weight. The values in the orbit graphs indicate the maximum and minimum limits given by the bearing support structure with a radial clearance of $0.5mm$.

Figure 10a shows the measured orbit in the bearings for a speed of 2000 RPM. An increase in amplitude is noticed in relation to the static system case. The movement of the rotor remains in a range less than $0.1mm$ ($100\mu m$) for bearings A and B. Figure 10b for a speed of 3000 RPM, it was observed there is a decrease in the vibration amplitude of the rotor in the bearing in relation to the system with a rotation speed of 2000 RPM, remaining at around $0.050mm$ ($50\mu m$) for bearings A and B. The results show that the system kept the rotor position within the limit in a stable and satisfactory way. As the system always presents a residual unbalance, with an increase in the rotation speed the amplitudes suffer alterations. In this case, it presents a decrease in the position amplitude due to the increase of rigidity related to the increase of the rotation frequency.

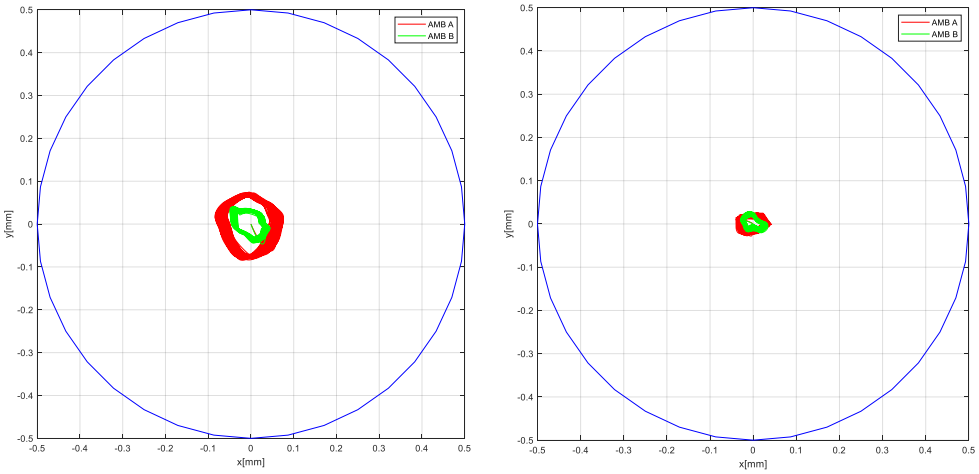

(a) 2000 RPM. (b) 3000 RPM.

Figure 10: Measured rotor orbits (in mm) at radial AMB locations at different spin speeds.

3.4 System response to unbalance excitation

Unbalance is a phenomenon characterized by a high amplitude at the peak of the rotation frequency. The behavior analysis takes into account some situations that can occur in reality. Thus, the results of the behavior of the system will be for excitation with general unbalance caused by two identical masses of $0.001kg$ positioned close to the bearings at a distance of $0.042m$ of the rotation axis of the rotor with phase angle is 120° as shown in Figure 11. The analysis will be done with the rotor rotating at rotation speeds of 2000 and 3960 RPM. A general unbalance is equivalent to a combination of static and dynamic effects, that is, the center of mass is outside the rotation axis and the main axis of inertia is inclined in relation to this. This combination implies a displacement of the center of mass and an inertia tensor with non-zero terms outside the main diagonal. The position of the new center of mass, known as eccentricity, given by a point mass that is outside the main rotor axis and outside the plane of

the central section of the rotor [19].

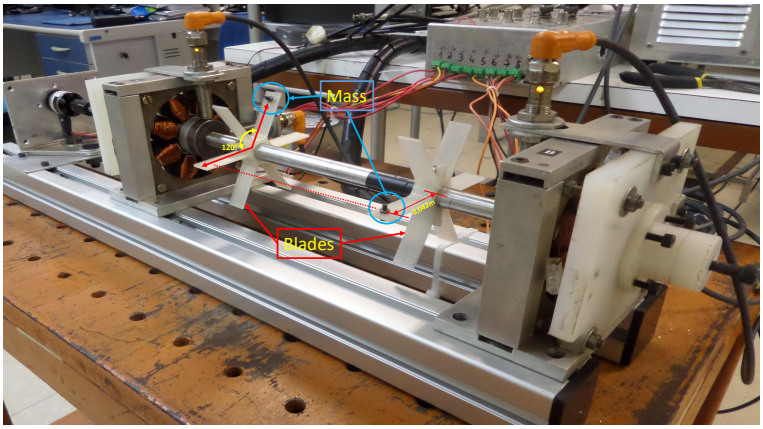

Figure 11: Test rig to General Unbalanced.

In the orbit of the Figure 12a for a sping speed of 2000 RPM, it is verified that the system presents a satisfactory response, remaining in a stable way, where the displacements remain with oscillations smaller than $0.30mm$ of amplitudes for both bearings. Figure 12b shows the behavior of the system with an increase in spin speed of approximately 3960 RPM. This maximum spin speed was restricted to the mechanical coupling of the motor, which induced considerable forces on the bearing. Nevertheless, the system presented a satisfactory response within the limit determined by the support bearings, remaining stable with oscillations smaller than $0.2mm$ of amplitude in the bearings. Note that there is a decrease in amplitude concerning the previous case (Figure 12a), due to the increase in stiffness related to the increase in the rotation frequency.

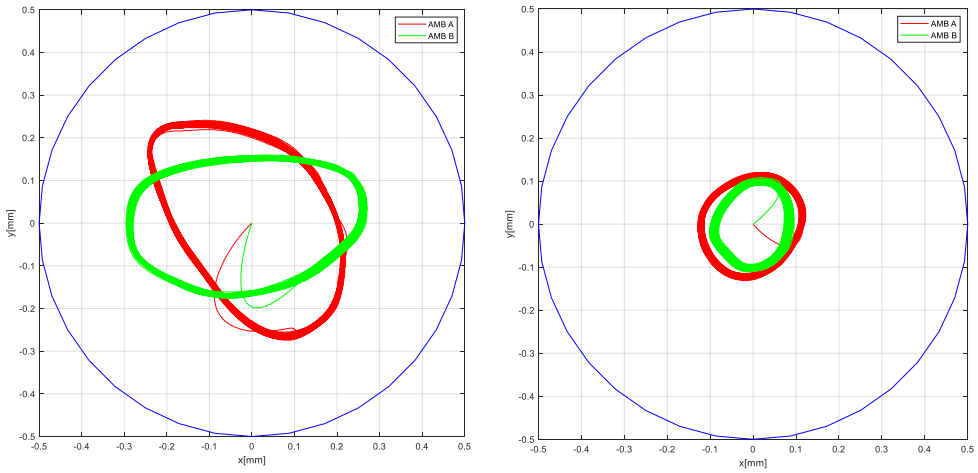

(a) 2000 RPM. (b) 3960 RPM.

Figure 12: Rotor orbit on AMBs with general unbalance.

4 Conclusions

In this study, the construction and operation of an AMB system for rotor levitation and stability are presented and discussed. The project presented satisfactory results with low vibration amplitudes and within the established limit, even without a mechanical precision in relation to alignment and centering that had little effect on the system's operation.

The experimental results were presented and discussed in several situations for the dynamic behavior of the system, such as the rotor in static, transient and rotor in steady-state driven by a DC motor. In the stationary regime, the system presented low amplitude in the measurements of the rotor positions. During the transient, the system responded satisfactorily, remaining stable. In the steady-state with motor activation, the results were adequate since there was an increase in amplitude, due to the tests that were carried out with the influence of loads. Despite this, the shaft remained within the design limits by levitating and turning.

References

[1] M. Aenis, E. Knopf, and R. Nordmann. Active magnetic bearings for the identification and fault diagnosis in turbomachinery. *Mechatronics*, 12(8):1011 – 1021, 2002.

[2] B. Aeschlimann, M. Hubatka, R. Stettler, and R. Housseini. Commissioning of off-shore gas compressor with 9-axes magnetic bearing system: Commissioning tools. In *15th International Symposium on Magnetic Bearings*, volume 9, pages 215–221, 2017.

[3] Angelo Bonfitto, Ran Gabai, Andrea Tonoli, Luis Miguel Castellanos, and Nicola Amati. Resonant inductive displacement sensor for active magnetic bearings. *Sensors and Actuators A: Physical*, 287:84–92, 2019.

[4] Rakesh P. Borase, D. K. Maghade, S. Y. Sondkar, and S. N. Pawar. A review of PID control, tuning methods and applications. *International Journal of Dynamics and Control*, (June), 2020.

[5] E.A. Costa, I. E. Chabu, and J. J Cruz. Application of active magnetic bearing for tubular linear induction motor in oil pumping. *Proceeding 11th International symposium on magnetic bearing*, August 2008.

[6] Michael I. Friswell, John E. T. Penny, Seamus D. Garvey, and Arthur W. Lees. *Dynamics of Rotating Machines*. Cambridge University Press, New York, 1 edition, 2010.

[7] Giancarlo Genta. Kinetic energy storage: an ideal application for magnetic bearings. *Proceedings of the 14th International Symposium on Magnetic Bearings (ISMB)*, August 2014.

[8] Oswaldo Horikawa, Rogério I. Yamamoto, and Isaías da Silva. Development of single axis controlled attraction type magnetic bearing and its application in ventricular assist device. *1st Brazilian Workshop on Magnetic Bearings*, Outubro 2013.

[9] JDrones. Arducopter motor. Acessado em 05/06/2020.

[10] Zbigniew Kozanecki, Małgorzata Gizelska, and Dorota Kozanecka. Monitoring and diagnostics of the rotating system with an active magnetic bearing. 198:547–552, 2 2013.

[11] S. Liu, D. Li, W. Yu, and J. Guo. Stiffness analysis of the magnetic bearing system. *Proceedings of the 9th International Symposium on Magnetic Bearings (ISMB)*, August 2004.

[12] Agnieszka Muszynska. *Rotordynamics*. CRC Press, New York, 1 edition, 2005.

[13] G. Rata, M. Rata, and C. Prodan. Analysis of the deforming regime generated by different light sources, using reconfigurable system - compactrio. pages 748–751, Oct 2014.

[14] Gerhard Schweitzer and Eric H. Maslen. *Magnetic Bearings - Theory, Design an Application to Rotating Machinery*. Springer-Verlag, Berlin, 1 edition, 2009.

[15] R. S. Siqueira. Projeto e implementação de um mancal magnético ativo com controle por modos deslizantes. Dissertação de Mestrado - UFRJ - COPPE/PEM - Programa de Pós-graduação em Engenharia Mecânica, 2013.

[16] Joaquim Siva, François Carrere, and Frédéric Ponson. Subsea gas compression station: Collaborative design using multiphysics/multiscale system simulation applied to active magnetic bearings. *1st Brazilian Workshop on Magnetic Bearings*, Outubro 2013.

[17] A Smirnov, Nikita Uzhegov, Teemu Sillanpää, Juha Pyrhönen, and Olli Pyrhönen. Design and evaluation of high-speed solid rotor induction machine supported by AMBs with a multidisciplinary tool. *15th International Symposium on Magnetic Bearings*, pages 467–473, 2016.

[18] Sparkfun. Sparkfun - monster moto shield. Acessado em 02/05/2020.

[19] Richard M. Stephan, Fernando A. N. Castro Pinto, Fernando Celso D. N. Gomes, José A. Santisteban, and Andres Ortiz Salazar. *Mancais Magnéticos - Mecatrônica sem atrito*. Editora Ciência Moderna, Rio de Janeiro, 1 edition, 2013.

[20] Se Young Yoon, Zongli Lin, and Paul E. Allaire. *Control of Surge in Centrifugal Compressors by Active Magnetic Bearings*. Springer-Verlag, London, 1 edition, 2013.